Original Paper

phys. stat. sol. (a) **204**, No. 3, 881–886 (2007) / **DOI** 10.1002/pssa.200622352

Recovery of dry etch-induced damage of nano-patterned GaN-based light-emitting diodes by rapid-thermal-annealing

Hyun-Gi Hong[1], **S.-S. Kim**[1], **D.-Y. Kim**[1], **Takhee Lee**[1], **Kyoung-Kook Kim**[2], **June-O. Song**[2], **J. H. Cho**[2], and **Tae-Yeon Seong**[*, 3]

[1] Department of Materials Science and Engineering, Gwangju Institute of Science and Technology, Gwangju 500-712, Korea
[2] Photonics program team, Samsung Advanced Institute of Technology, Suwon 440-600, Korea
[3] Department of Materials Science and Engineering, Korea University, Seoul 136-713, Korea

Received 21 July 2006, revised 17 October 2006, accepted 18 October 2006
Published online 14 December 2006

PACS 73.61.Ey, 78.60.Fi, 81.16.Rf, 85.60.Bt, 85.60.Jb

The effect of rapid-thermal-annealing on the performance of near-UV GaN-based light-emitting diodes (LEDs) fabricated with nano-patterned p-type electrodes has been investigated. One-dimensional (1-D) nano-patterns were formed on Cu-doped indium oxide (CIO)/indium tin oxide (ITO) p-electrode by surface relief grating and dry etching techniques. After the nano-patterning, some of the samples are rapid-thermal-annealed at 530 and 630 °C in either air or nitrogen ambient. LEDs made with samples annealed 530 °C show much better electrical characteristics as compared to unannealed samples. In particular, LEDs with samples annealed 530 °C in air show higher output power (at 20 mA) and much reduced leakage current as compared to LEDs with unannealed samples.

GaN-based light-emitting diode (LED) technology is of great importance for its application to solid-state lighting [1]. For solid-state lighting application, the enhancement of light extraction efficiency of GaN-based LEDs is one of the major technological issues to be resolved, because external quantum efficiency is relatively low as compared to internal quantum efficiency. This is in part due to high refractive indices (>2) of GaN and ITO p-type current spreading electrodes, which cause most of the emitted light to be trapped inside the device [2, 3]. To increase the light extraction, various methods were used, such as the surface roughening and patterning of p-electrodes, which produce sidewalls near the surface, through which the light inside the device can escape [2–7]. For example, Hong et al. [2, 3] investigated the one-dimensional (1-D) and two-dimensional (2-D) nano-patterning of Cu-doped indium oxide (CIO)/indium tin oxide (ITO) electrodes and showed that the patterned LEDs give the improvement of the light output by about 40% as compared with unpatterned LEDs. In addition, Wierer et al. [5] introduced photonic crystal structure to enhance the light output of LEDs. These patterning and roughening methods reported so far were processed with a dry etching technique, which have several advantages, such as good selectivity, anisotropy, and a clean process. However the dry etching technique could introduce etch damage to devices [6, 8–11]. For example, dry etching could cause lattice defects to be generated near LED sidewalls, which offer leakage current paths, and so increase reverse leakage current, i.e., the degradation of device reliability. In order to recover such damages, thus, various methods of plasma treatment and thermal annealing have been introduced [8–10]. In this work, we have one-dimensionally patterned CIO/ITO p-type electrodes using a surface relief grating (SRG) method combined with a dry etching process [2, 3]. In order to recover etch damage, the patterning was followed by rapid-thermal-annealing

[*] Corresponding author: e-mail: tyseong@korea.ac.kr

in different ambient (either air or nitrogen). It is shown that annealing in air is very effective in improving the electrical properties of LEDs.

GaN-based near-UV (405 nm) LED structures were grown using a metalorganic chemical vapor deposition (MOCVD) system. The LED structures were comprised of a GaN buffer layer, n-GaN, an InGaN/GaN multi-quantum well active layer and p-GaN. LEDs mesa-structures (300 μm × 300 μm in size) were defined by means of dry etching. The CIO(3 nm)/ITO(400 nm) p-contact layers were deposited on p-GaN by e-beam evaporation [12]. After lift-off, the LEDs were annealed at 630 °C for 1 min in air. After fabricating full mesa LED structures, an 1-D TiO_2 etch mask was formed using surface relief grating (SRG) and sol-gel techniques. The detail of the SRG process was published elsewhere [13]. The ITO layer was then selectively etched using the 1-D TiO_2 etch mask by means of inductively coupled plasma etching (ICP). The etching was conducted in Ar and CH_4 plasma and the etching depth of the ITO was 100 nm. The flow rate of Ar and CH_4 gases was controlled to 54 and 6 sccm, respectively, and ICP power was controlled to 1000 W. Finally, the 1-D TiO_2 nano-mask was selectively removed by reactive ion etching (RIE) in CF_4 plasma. After the 1-D nano-patterning process, some of the samples were rapid-thermal-annealed at 530 and 630 °C in either air or nitrogen ambient. Morphology of the 1-D nano-patterned ITO electrodes of LEDs was examined by atomic force microscopy (AFM, PSIA, XE-100). Current–voltage (*I–V*) characteristics of LEDs were investigated using a parameter analyzer (HP4155A). Their output powers were also characterized.

Figure 1 shows AFM images of an 1-D nano-patterned ITO layers before and after rapid-thermal-annealing. For the samples annealed at 530 °C in either air or N_2-ambient, Fig. 1(a) and (b), respectively, the patterned structures remain stable, which is comparable to that of the unannealed sample (Fig. 1(c)). The patterned structures are 500 nm in periodicity, 200 nm in width, and 100 nm in depth. The spacing between the individual patterns is measured to be 300 nm. For the sample annealed at 630 °C in air, Fig. 1(d), however, the patterned structures is almost completely deformed; Individual patterns seem to be grown up, so leading to the reduction of sidewalls. The sample annealed at 630 °C in

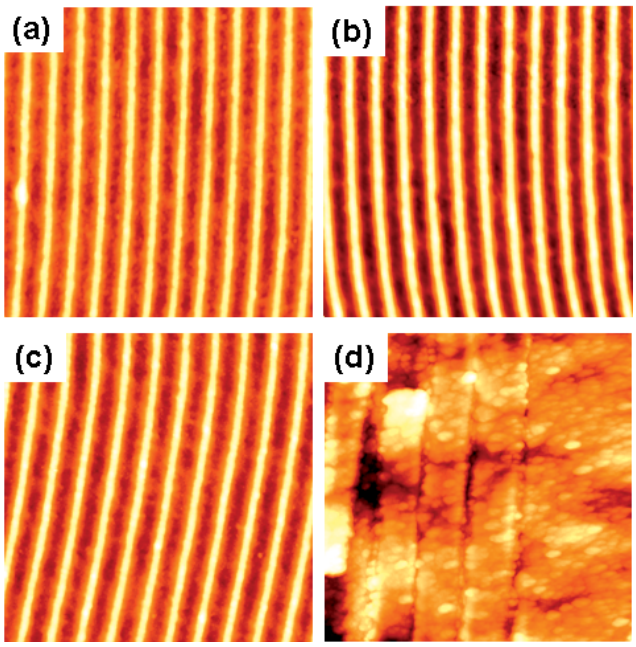

Fig. 1 (online colour at: www.pss-a.com) AFM images (5 μm × 5 μm) of the 1-D nano-patterned ITO layers. Annealed at 530 °C in either (a) air-ambient or (b) N_2-ambient; (c) unannealed; (d) annealed at 630 °C in air.

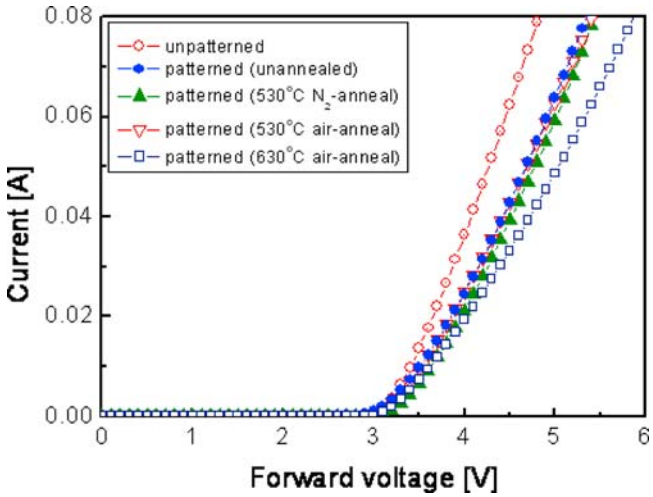

Fig. 2 (online colour at: www.pss-a.com) Forward $I-V$ characteristics of LEDs fabricated with the CIO(3 nm)/ITO(400 nm) p-contact layers before and after patterning.

N_2-ambient (not shown in Fig. 1) revealed the pattern similar to that of the sample annealed at 530 °C in air. However, the sample became almost opaque.

Figure 2 shows the forward $I-V$ characteristics of LEDs fabricated with the CIO(3 nm)/ITO(400 nm) p-contact layers before and after patterning. The patterned LEDs produce higher forward bias voltages as compared with the unpatterned sample. This could be attributed to reduction of the surface area of the contact layer, which is in contact with a probe tip for power-supply. It is shown that regardless of the annealing ambients used, the patterned samples annealed at 530 °C give similar $I-V$ characteristics. However, annealing the sample at 630 °C in air leads to the degradation of $I-V$ behaviour due to the deformed surface pattern of the p-type electrode [12], as shown in Fig. 1(d).

Figure 3 shows the reverse leakage characteristics of LEDs made with the CIO/ITO p-contact layers before and after patterning. It is shown that the patterned LED produce fairly high reverse leakage cur-

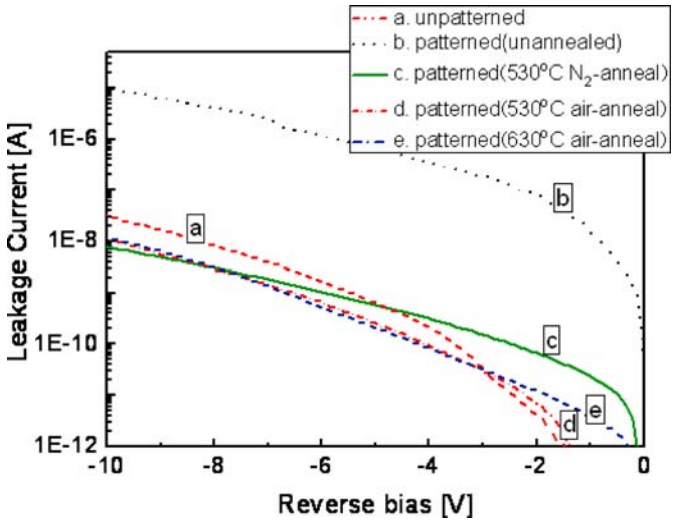

Fig. 3 (online colour at: www.pss-a.com) Reverse leakage characteristics of LEDs made with the CIO/ITO p-contact layers before and after patterning.

Table 1 Summary of electrical properties of LEDs fabricated with different p-type electrodes.

sample	V_f at 20 mA (V)	series resistance (Ω)	I_r at –10 V (10^{-5} A)
unpatterned	3.65	19.6	0.0312
patterned (unannealed)	3.86	23.7	1
patterned (530 °C, annealed in N_2)	3.97	24.8	0.0078
patterned (530 °C, annealed in air)	3.85	24.16	0.0116
patterned (630 °C, annealed in air)	4.03	30.7	0.012

V_f and I_r denote forward bias voltage and reverse leakage current, respectively.

rent. However, the leakage current of the patterned LEDs is dramatically reduced upon rapid-thermal-annealing, which is comparable to that of the unpatterned sample. For example, annealing of the patterned samples results in the reduction of the reverse leakage current at –10 V by about two orders of magnitude, compared with that of the unannealed sample. The electrical characteristics of the LEDs are summarized in Table 1. This indicates that post-patterning annealing is very effective in recovering dry-etch-induced damage. In other words, etch-induced lattice defects are annihilated effectively by annealing, resulting in the reduction of the reverse leakage current.

Figure 4 shows the transmittance of ITO films before and after annealing in either air or N_2 ambient. The air-annealed and unannealed ITO films show higher transmittance in the range of 400–500 nm than the N_2-annealed sample. For example, the unannealed, air-annealed, and N_2-annealed samples show transmittance of 79, 79 and 60% at a wavelength of 405 nm, respectively. The exact reason why the N_2-annealed sample gives low transmittance is not clear at the moment. The low transmittance may be attributed to an increase of defects such as oxygen vacancy, which cause ITO to have metallic properties [14].

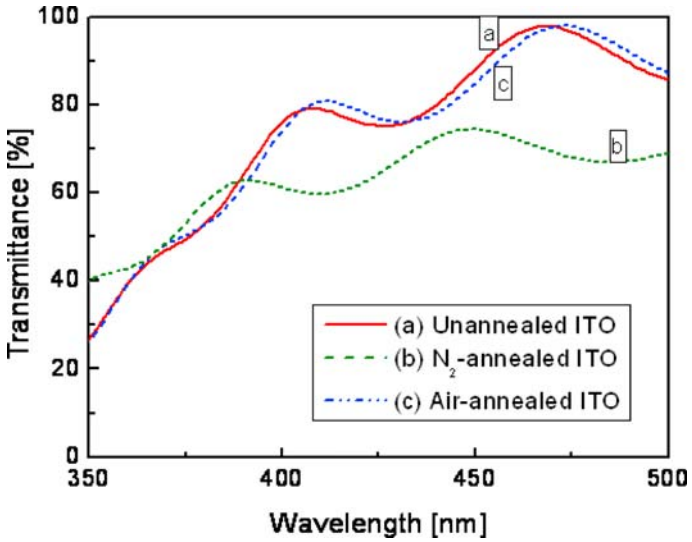

Fig. 4 (online colour at: www.pss-a.com) Transmittance of ITO films before and after annealing in either air or N_2 ambient.

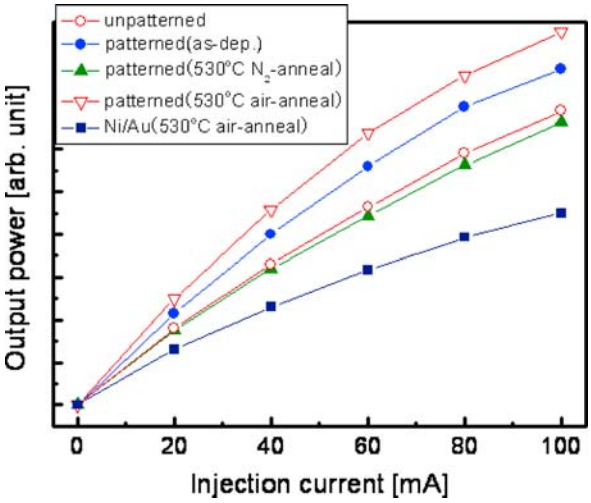

Fig. 5 (online colour at: www.pss-a.com) Light output–current (L–I) characteristics of LEDs before and after patterning as a function of the forward drive current. It is shown that the patterned LEDs before and after annealing at 530 °C in air give much higher light output power compared to that of the unpatterned sample.

Figure 5 shows the light output–current (L–I) characteristics of LEDs before and after patterning as a function of the forward drive current. It is shown that the patterned LEDs before and after annealing at 530 °C in air give much higher light output power compared to that of the unpatterned sample. For example, the LEDs with the patterned p-contact layer after air-annealing show the improvement of the output power at 20 mA by 16% and 88% as compared with the LEDs with unannealed samples and conventional Ni(5 nm)/Au(5 nm) p-contact layers, respectively. The patterning-induced increase of the output power can be explained in terms of the generation of additional sidewalls near the surface and light extraction through the side walls. However, the patterned sample annealed in N_2 ambient shows poor light output even lower than that of the unpatterned sample. This degradation seems to be caused by the low transmittance of the p-type electrodes, as shown in Fig. 4.

In conclusion, we have introduced a rapid thermal annealing technique to recover the etch-induced damage of the 1-D patterned near-UV LEDs. It was shown that compared with unannealed samples, the patterned LEDs exhibit reduced reverse leakage current by two orders of magnitude when annealed at 530 °C. Furthermore the patterned LEDs produced much improved light output performance as compared with the unannealed sample. The result implies that the post-RTA process could be of technological importance for the fabrication of highly reliable patterned near-UV LEDs.

Acknowledgement This work was supported by the basic research program of the Korea Science & Engineering Foundation (Grant no. R01-2006-000-10904-0).

References

[1] D. A. Steigerwald, J. C. Bhat, D. Collins, R. M. Fletcher, M. O. Holcomb, M. J. Ludowise, P. S. Martin, and S. L. Rudaz, IEEE J. Sel. Top. Quantum Electron. **8**, 310 (2002).
[2] H.-G. Hong, S.-S. Kim, D.-Y. Kim, T. Lee, J.-O. Song, J. H. Cho, C. Sone, Y. Park, and T.-Y. Seong, Appl. Phys. Lett. **88**, 103505 (2006).
[3] H.-G. Hong, S.-S. Kim, D.-Y. Kim, T. Lee, J.-O. Song, J. H. Cho, C. Sone, Y. Park, and T.-Y. Seong, Semicond. Sci. Technol. **21**, 594 (2006).
[4] D.-S. Leem, J. H. Cho, C. Sone, Y. Park, and T.-Y. Seong, J. Appl. Phys. **98**, 076107 (2005).
[5] J. J. Wierer, M. R. Krames, J. E. Epler, N. F. Gardner, M. G. Craford, J. R. Wendt, J. A. Simmons, and M. M. Sigalas, Appl. Phys. Lett. **84**, 3885 (2004).
[6] R.-H. Horng, C. C. Yang, J. Y. Wu, S. H. Huang, C. E. Lee, and D. S. Wuu, Appl. Phys. Lett. **86**, 221101 (2005).
[7] T. Fujii, Y. Gao, R. Sharma, E. L. Hu, S. P. Denbaars, and S. Nakamura, Appl. Phys. Lett. **84**, 855 (2004).

[8] X. A. Cao, S. J. Pearton, A. P. Zhang, G. T. Dang, F. Ren, R. J. Shul, L. Zhang, R. Hickman, and J. M. Van Hove, Appl. Phys. Lett. **75**, 232 (1999).
[9] X. A. Cao, S. J. Pearton, A. P. Zhang, G. T. Dang, F. Ren, R. J. Shul, L. Zhang, R. Hickman, and J. M. Van Hove, Appl. Phys. Lett. **75**, 2569 (1999).
[10] J.-M. Lee, C. Huh, D.-J. Kim, and S.-J. Park, Semicond. Sci. Technol. **18**, 530 (2003).
[11] R. J. Shul, M. L. Lovejoy, D. L. Hetherington, D. J. Rieger, J. F. Klem, and M. R. Melloch, J. Vac. Sci. Technol. B **13**, 27 (1995).
[12] J.-O. Song, J. S. Kwak, Y. Park, and T.-Y. Seong, Appl. Phys. Lett. **86**, 213505 (2005).
[13] S.-S. Kim, C. Chun, J.-C. Hong, and D.-Y. Kim, J. Mater. Chem. **16**, 370 (2006).
[14] R. X. Wang, C. D. Beling, S. Fung, A. B. Djurisic, C. C. Ling, and S. Li, J. Appl. Phys. **97**, 033504 (2005).

